A Novel Twin-Shaft Rotor with Active Magnetic Couplings for Vibration Control

Chris Lusty[a], Necip Sahinkaya[a,b], Patrick Keogh[a]

[a] University of Bath, Claverton Down, Bath, UK, C.Lusty@bath.ac.uk
[b] School of Mechanical Engineering, Kingston University, London, UK

***Abstract*—A novel rotor topology is proposed with the goal of reducing vibration in high speed rotor systems. Primarily, reduction in synchronous vibration at critical speeds is targeted. In essence, the novel topology consists of a hollow tube rotor coupled to a secondary non-rotating shaft through a number of actively managed magnetic couplings. An outline of the new topology is provided, along with a finite element analysis comparing the out-of-balance vibration response of the proposed rotor to a comparable simple rotor. Designs for a test rig based on this topology are presented, together with an outline of anticipated testing and potential future development of the idea.**

I. Introduction

In order to alter the vibration characteristics of a rotor, it is proposed to use a novel arrangement of components coupled with active control. The key principle of the concept is to include, in addition to the primary rotor, a secondary "damping shaft". This second shaft runs concentrically through the primary rotor (which must naturally be hollow) and does not rotate. The two shafts are independently supported - the primary rotor on some form of bearing (e.g. rolling element), and the secondary shaft simply clamped.

Mounted along the length of the secondary shaft are one or more magnetic bearings. These magnetic bearings are "inside-out" compared to standard magnetic bearings, in that the stator is on the inside, and the rotor on the outside. In ordinary low speed operation of the rotor (i.e. when vibration is not a problem), these magnetic bearings are not activated, and thus there is no link whatever between the two shafts of the system. However, as critical speeds are approached by the rotor, the magnetic bearings can be activated, coupling the two shafts and changing the vibration behaviour of the rotor.

By altering the axial position and/or number of magnetic bearings activated at any given time, the overall system characteristics can be altered, and thus a variety of frequencies of vibration mitigated. Via active control, it is therefore anticipated that such a system will offer a powerful and flexible way to control excessive vibration.

II. Prior Work in Similar Areas

A good overview of the mechanisms leading to synchronous rotor vibration is provided by Nelson [1]. Reducing vibration amplitudes theoretically permits higher speed applications, and thus smaller, higher power density machines. From a research point of view, active rotor vibration reduction techniques may be considered to split into three distinct groups:

1. Those concerned with active balancing, i.e. redistributing mass around the rotor system to remove the driving force of synchronous vibration. These methods tend to be adaptations of off-line balancing methods. Such techniques have been a topic of interest since Van de Vegte's paper [2] proposing the design of an active balancing head. Various developments in both control logic and physical design have been presented since [3]–[8]. A good review of this field is provided by Zhou and Shi [9].

2. Those concerned with directly applying forces to the rotor; generally this is by means of lateral forces either at the supporting bearings or mid-span along the shaft. Direct force application methods are primarily the domain of the magnetic bearing. Much work has been done on optimising the control strategies for the bearings to minimise vibration, but they are necessarily limited in their performance by constraints of physical size and load capacity. The function and application of magnetic bearings is comprehensively considered by Maslen and Schweitzer [10], with a recent review paper of research topics in the field provided by Schweitzer [11]. Other types of active bearing have also been considered, including squeeze film dampers, gas bearings and laterally actuated passive bearings [12]–[15].

In terms of applying forces at mid-span (i.e. non-bearing) locations, a significant amount of research has been done surround the concept of the Active Magnetic Damper (AMD). An early example is provided by Nikolajsen *et al.* [16], who model a marine propulsion shaft, one of whose members rotates super-critically. By applying an AMD to this shaft, Nikolajsen demonstrates substantial reduction of synchronous vibration amplitude. Nikolajsen's work was extended by Kasarda *et al.* [17] with the addition of disks to an otherwise simple rotor. Kasarda proves that not only does an AMD have significant scope to reduce the amplitude of the vibration, but also that the exact placement of the AMD is not critical to its successful performance. Particular comparison is drawn between locating the AMD near mid-span (i.e. point of maximum deflection for first mode vibration), near a disk not at mid span, and close to one of the supporting bearings. In a later paper, Kasarda *et al.* [18] focus on the potential for AMDs to be used in the control of sub-synchronous vibrations cause by external influences.

The common theme throughout all of the research presented on AMDs is that they are external-stator devices, and they are

rigidly fixed to the ground/machine base. This differs from the work presented in this paper, which uses internal-stator bearings mounted on a flexible support shaft.

3. Those that are less clearly defined in nature. Techniques here generally involve changing some physical property of the system (other than mass redistribution), for example stiffness or geometry, and thus alter vibration response.

The technique proposed in this paper falls somewhere between this category and the "direct force application" category (2). Here the aim is to alter the definition of the rotor system in such a way as to bypass vibration peaks, which involves an element of lateral force application to the rotor. A previous attempt at geometry-alteration method is presented by Ortega *et al.* [19], where it is proposed to axially move one of the support bearings in order to change the rotor's effective length. Conversely this paper advocates activating *additional* bearings at other axial locations.

III. The Proposed Topology

Figure 1 shows a simplified illustration of the proposed rotor layout. The rotor is a hollow tube of soft magnetic metal (e.g. steel) supported on external rolling element, or other passive bearings. The damping shaft is supported entirely separately by non-rotating supports, either pin-jointed or clamped. The material for the non-rotating shaft is chosen on a basis of its stiffness qualities, and it need not have appreciable magnetic permeability. The fact that this shaft does not rotate gives the advantage that any imbalance present in the member does not add to or complicate the dynamics of the primary rotor when the two shafts are coupled. The active couplings are achieved by internal-stator magnetic bearings. A cross sectional view of one of these is provided in Figure 2.

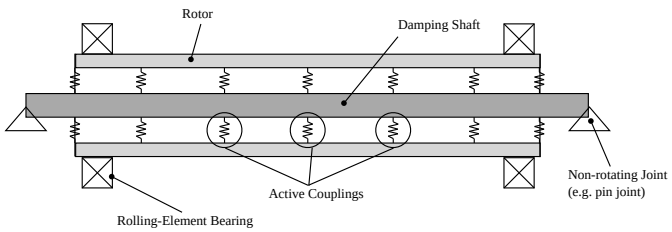

Figure 1. Schematic view of proposed novel rotor topology. Note that the number/position of "active couplings" is arbitrary.

IV. Magnetic Bearing Considerations

In addition to the new ideas regarding rotor topology presented here, significant consideration is given to the magnetic bearings that are to form the active coupling element between the shafts. In the vast majority of magnetic bearing systems used today, the stator of the bearing is outside of the rotor (external stator systems). This arrangement is chosen because it removes size constraints from the design of the stator allowing more powerful bearings to be designed. It is clearly also infeasible to use internal stator bearings on either solid shafts or very thin shafts. However, the external stator does

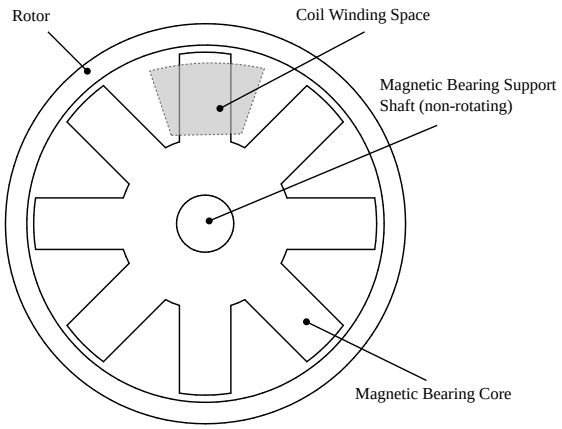

Figure 2. Schematic cross-section of internal magnetic bearing

have disadvantages. It takes up significant space along the shaft's length that may otherwise be either used for mounting other components. Furthermore, in certain applications there may not be space in the vicinity of the shaft to use an external stator bearing.

The design presented here uses custom designed internal stator magnetic bearings. In addition to addressing the space issues presented by by external stator bearings, the circumstance of the internal bearings being mounted on a flexible shaft is central to the design and exploits possibilities relating to the overall system dynamics not considered by other work on active magnetic damping.

A. Stator Core Material

It is almost universal practice in magnetic bearing design to construct the cores out of laminated electrical steel. This provides a high level of magnetic permeability and good saturation strength, while reducing energy losses due to eddy current build up. However, design geometry possibilities are considerably limited when working with laminated steel. In particular, to facilitate manufacture it is desirable for the design to be prismatic in the stacking direction (to enable every individual lamination to be identical). It is well documented that this requirement makes the manufacture of homopolar magnetic bearings more complex and costly than heteropolar designs. Indeed despite the fact that homopolar designs incur lower eddy current losses than heteropolar arrangements, the difficulty of manufacture leads to the majority of magnetic bearings using the less efficient, but easier to manufacture, heteropolar layouts.

To overcome this trade off, it is proposed that laminated steel is replaced with a powder metal based Soft Magnetic Composite (SMC) as the core material for a magnetic bearing. SMC offers several clear advantages over laminated steel:

- It has effectively isotropic lamination and is thus capable of supporting alternating magnetic flux in any direction without eddy current build up
- It has the ability to be formed into complex 3D shapes

For this project, the adoption of SMC allows the magnetic bearings to use a compact, single piece homopolar design sim-

ilar to that shown in Figure 3. Fabricating this design directly from laminated steel would incur greater eddy current losses than an SMC core as not all directions are insulated in the steel. Fabricating a comparable equally compact homopolar core in a fully insulated way from a multi-part laminated steel design would be substantially more complex.

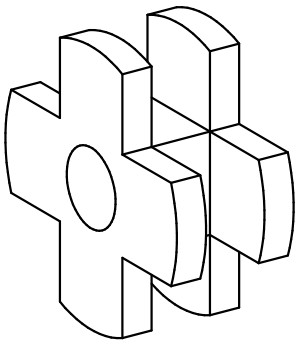

Figure 3. An internal-stator homopolar bearing core

In general, SMC is fabricated from iron powder, chemically treated to leave each individual grain with a thin layer of electrically insulating material around the outside. The powder is then compressed in a mold to form the final shape of the component required. Post forming heat treatments are also applied to relieve stress from the compaction process.

Of course, the compaction-forming of powder-metal components is generally only financially viable on production scale runs, not for small/one-off jobs. For this reason, prefabricated discs of a version of the SMC material specially treated to have good machinability properties are used. It is noteworthy that in altering the material to give good machinability, the magnetic properties of the SMC are slightly adversely affected.

Of course, one still has the issues of space limitation when designing an internal-stator magnetic bearing. In general this means one is limited by the load capacity of the bearing. This is, however, by no means a prohibitive difficulty in this design, owing to the fact that the bearings are not required to support the mass of the rotor (which is dealt with by external rolling element bearings).

V. Numerical Modelling

A. Finite Element Model

The following derivation is based on standard Finite Element rotor modelling, described by Nelson [20]. The basic unit of the finite element model used is an eight degree-of-freedom rotor section having degrees-of-freedom collected into a single vector:

$$\mathbf{q}(t) = (x_1(t), y_1(t), \theta_1(t), \phi_1(t), x_2(t), y_2(t), \theta_2(t), \phi_2(t))^T$$

where (x_i, y_i) are node lateral displacement, and (θ_i, ϕ_i) are node angular displacements.

The element equation of motion has the form:

$$\mathbf{m}\ddot{\mathbf{q}} - \Omega\mathbf{g}\dot{\mathbf{q}} + \mathbf{k}\mathbf{q} = \mathbf{f} \tag{1}$$

Here $\mathbf{m}$, $\mathbf{k}$ and $\mathbf{g}$ are mass, stiffness and gyroscopic matrices respectively. $\mathbf{f}$ is a column vector of forces applied to each of the degrees of freedom in $\mathbf{q}$. Ω is the speed of shaft rotation (rad/s).

The complete equation of motion for a multi-element rotor is:

$$\mathbf{M}\ddot{\mathbf{Q}} - \Omega\mathbf{G}\dot{\mathbf{Q}} + \mathbf{K}\mathbf{Q} = \mathbf{F} \tag{2}$$

where $\mathbf{M}$, $\mathbf{K}$, $\mathbf{G}$, $\mathbf{F}$ and $\mathbf{Q}$ are the global equivalents of the elemental terms $\mathbf{m}$, $\mathbf{k}$, $\mathbf{g}$, $\mathbf{f}$ and $\mathbf{q}$, respectively.

This is fairly standard analysis in rotor dynamics. From this point, modelling of the coupled shaft system is undertaken as follows. Firstly, the $\mathbf{Q}$ vector is extended to include degrees of freedom for both the rotor ($\mathbf{Q_R}$) and the secondary shaft ($\mathbf{Q_S}$):

$$\mathbf{Q} = \begin{bmatrix}\mathbf{Q_R} & \mathbf{Q_S}\end{bmatrix}^T$$

Using this definition, an expanded form of Equation (2) is presented, which demonstrates where coupling terms are applied between the two shafts:

$$\begin{bmatrix}\mathbf{M_R} & \mathbf{0} \\ \mathbf{0} & \mathbf{M_S}\end{bmatrix}\begin{bmatrix}\ddot{\mathbf{Q}}_\mathbf{R} \\ \ddot{\mathbf{Q}}_\mathbf{S}\end{bmatrix} + \begin{bmatrix}\Omega\mathbf{G} & \mathbf{0} \\ \mathbf{0} & \mathbf{0}\end{bmatrix}\begin{bmatrix}\dot{\mathbf{Q}}_\mathbf{R} \\ \dot{\mathbf{Q}}_\mathbf{S}\end{bmatrix} + \dots$$
$$\dots \begin{bmatrix}\mathbf{K_R} + \mathbf{K_C} & -\mathbf{K_C} \\ -\mathbf{K_C} & \mathbf{K_S} + \mathbf{K_C}\end{bmatrix}\begin{bmatrix}\mathbf{Q_R} \\ \mathbf{Q_S}\end{bmatrix} = \begin{bmatrix}\mathbf{F_R} \\ \mathbf{F_S}\end{bmatrix} \tag{3}$$

Note that due to its non-rotation, there is no gyroscopic term for the secondary shaft. The $\mathbf{K_C}$ terms in Equation (3) represent the stiffness of the magnetic coupling between the two shafts.

Equation (3) is representative of the kind of coupling shown in Figure 1, i.e. simple spring couplings, and this is indeed the kind of coupling used in the results presented in this paper. However, due to the actively controlled nature of the magnetic bearings, it is possible to implement other forms of coupling. For instance, damping can be added by applying a control force proportional to the relative velocity, rather than the relative displacement, of the two shafts. This may be modelled by modifying the second matrix term in Equation (3) to:

$$\begin{bmatrix}\Omega\mathbf{G} + \mathbf{C_C} & -\mathbf{C_C} \\ -\mathbf{C_C} & \mathbf{C_C}\end{bmatrix}$$

where $\mathbf{C_C}$ includes a damping rate. For the present case however, the model is left as in Equation (3).

To achieve a frequency analysis of a rotor subject to any given forcing, one can take the Laplace transform of Equation (3), set $s = j\omega$, and rearrange into the form of:

$$\mathbf{Q}(j\omega) = (-\mathbf{M}\Omega^2 - \Omega^2\mathbf{G}j + \mathbf{K})^{-1}\mathbf{F}(j\omega) \tag{4}$$

It can be seen that for a specific rotor with a specific out of balance mass, all the terms on the right hand side of Equation (4) are known, and thus the response in the various degrees of freedom may be calculated.

B. Case Study

The application of this model to a particular system is now presented to illustrate the effectiveness of the internal shaft/magnetic bearing system. The rotor modelled is topologically as shown in Figure 1, with the difference that just a single magnetic bearing at the axial mid-point is used. The rotor is modelled as a 1 m long steel tube, of outside diameter 80 mm and wall thickness 2 mm. It is acknowledged that a 2 mm thickness would be insufficient to carry the full flux of the magnetic bearing at moderate to high field strengths, and thus an external steel collar at the bearing location would be needed in practice.

The inner (non-rotating) shaft used in the model is a 1.2 m long solid aluminium bar with a diameter of 20 mm. The supports for both rotor and secondary shaft are modelled as pin joints. The magnetic bearing is modelled to have a 1 mm clearance between its outer diameter and the inner diameter of the rotor giving a maximum force capability of 500 N and leading to a maximum available stiffness of 5×10^5 N/m.

A frequency response was calculated for this rotor with an arbitrary out-of-balance mass at a point along its length. For the first simulation, the rotor was entirely decoupled from the secondary shaft (magnetic bearing switched off). The simulation was then repeated with the magnetic bearing activated, and thus the two shafts coupled. Figure 4 shows both frequency responses. It is observed that the plot of the response of the uncoupled rotor includes two critical speeds at around 110 Hz and 440 Hz. These can easily be verified analytically using:

$$\omega_n = a_n \sqrt{\frac{EI}{\mu l^4}} \tag{5}$$

For a simply supported beam, a_n takes values of $(i\pi)^2$ for ω_i.

It is clear that the peak at $\simeq$ 110 Hz in the simple rotor response is absent in the coupled system response. Thus if the magnetic bearing is activated at, say 85 Hz, and then deactivated at around 165 Hz, that entire vibration peak is avoided. Note that the frequency responses are RMS averages of the responses at all nodes.

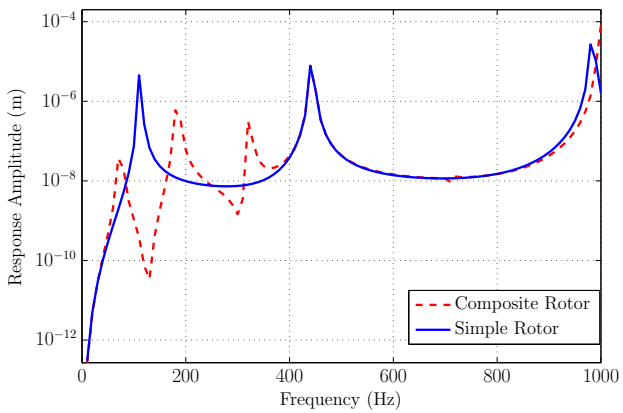

Figure 4. Vibration response to arbitrary out-of-balance mass on both simple and composite rotors (coupling at mid-span)

It is of interest to examine exactly what vibration, in the sense of mode shapes and amplitudes, the rotor (and secondary shaft, where relevant) is experiencing at key frequencies. For instance, if the magnetic bearing is activated at 90 Hz to circumvent the rotor's first critical speed as suggested by Figure 4, the response seen in Figure 5 is obtained. The amplitude of the rotor's vibration is much the same both before and after bearing activation, and it remains in a classic "first-mode" shape in both conditions. This agrees with this frequency being approximately the intersection of the two vibration responses shown in Figure 4. It is observed that the secondary shaft takes a shape having a combination of first and third modes. This may be explained by examining the natural frequencies of the shaft itself, calculated analytically via Equation (5). The shaft's second natural frequency (ignoring the effect of the magnetic bearing which will tend to reduce the value) is around 110 Hz. Of course the shaft is prevented from exhibiting any second mode vibration shapes by the fact that the excitation is applied at the centre - a node in all even mode shapes. Thus the combination is of first and third shapes.

At the first critical speed of the uncoupled rotor, 110 Hz, the mode shape diagram in Figure 6 reinforces just how much of an effect coupling to the second shaft has in terms of amplitude reduction. Indeed to see the shapes of the members when coupling is active, it is necessary to plot a separate zoomed-in figure of those responses, such is the difference in their relative scales. This is presented in Figure 7. It can be seen that the secondary shaft is once more vibrating with a combination of first and third modes, with increasing emphasis on the third mode as the exiting frequency nears the shaft's own third natural frequency.

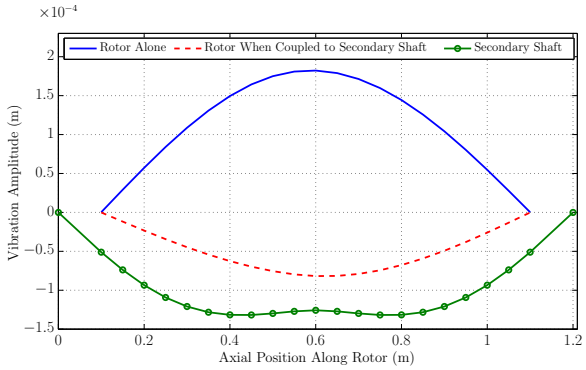

Figure 5. Response shapes at 90 Hz

It is noted that the arrangement for which Figure 4 shows the vibration response does not offer any avoidance of the second critical speed ($\simeq$ 440 Hz) as it does for the first. This is expected given that the mode shape of the second natural frequency or the rotor will have a node at central span, and thus a coupling located here is of no consequence whatever. This is the reason for proposing either multiple or mobile (or both) couplings. Figure 8 shows the frequency response of the exact same compound rotor, but this time with magnetic bearings activated near the $1/4$ and $3/4$ axial points rather than the centre. This arrangement allows for successful avoidance of the second resonant peak in the simple rotor response. In this

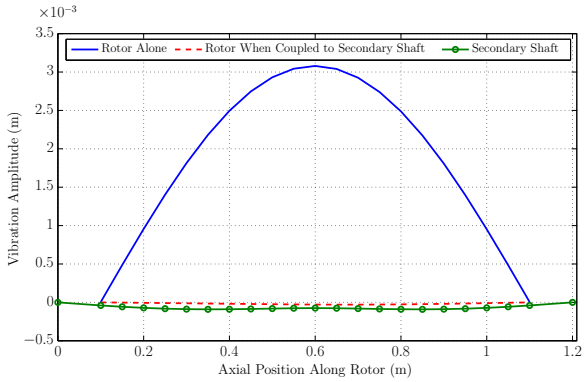

Figure 6. Response shapes at 110 Hz

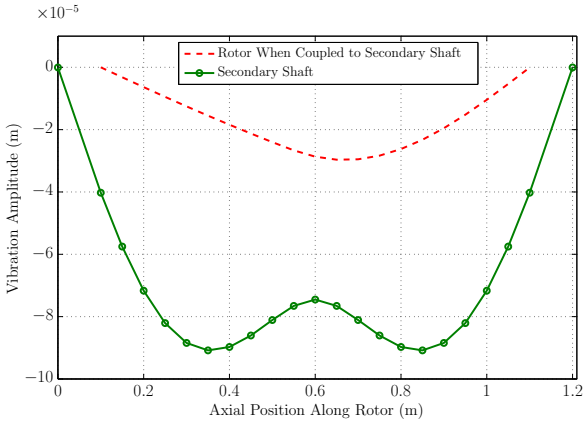

Figure 7. Response shapes at 110 Hz - magnification to show coupled member shapes

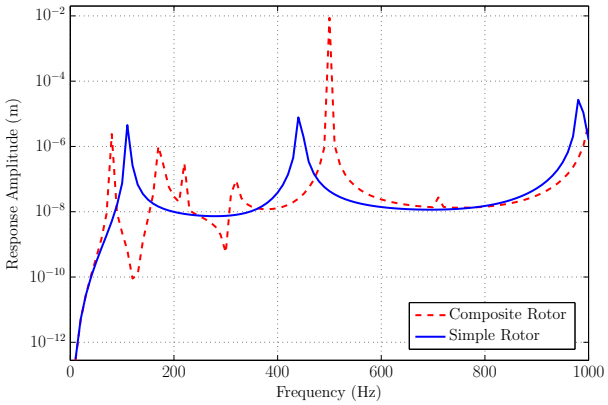

Figure 8. Vibration response to arbitrary out-of-balance mass on both simple and composite rotors (coupling around 1/4 and 3/4 axial points)

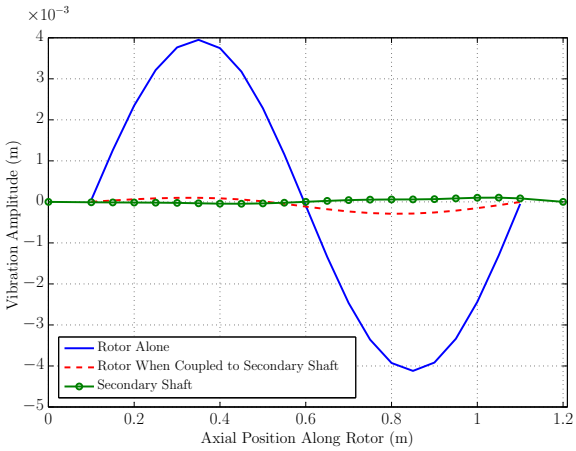

Figure 9. Mode Shapes at 440 Hz with 1/4 and 3/4 point coupling

model, it is apparent that such coupling also allows avoidance of the first critical speed. A mode shape plot is provided for the system at 440 Hz in Figure 9. One clearly sees the second mode shape of the rotor vastly decreased in amplitude by the coupling. Note that the slight asymmetry observable in the mode shape plots can be attributed to the fact that the out of balance mass being simulated is applied to an off-centre node in the finite element model (to allow symmetric mode shape responses to be observed).

C. Motion of Inner Shaft

A question arises regarding the stiffness and/or motion of the inner shaft. Namely, it is vital to ensure that no contact will occur between the rotor and the magnetic bearing. It is noted that providing the displacement of the central shaft relative to the displacement of the rotor does not cause a collision between the magnetic bearing and the rotor, it is permissible for this shaft to vibrate.

To address the collision concern, an out-of-balance mass is simulated on the rotor, and the amplitude of the displacement of the magnetic bearing relative to the corresponding (adjacent) location of the rotor is plotted. When considering the resultant plot shown in Figure 10, two facts are borne in mind. Firstly, at rest there is designed to be a 1 mm gap between the AMB and the rotor, and secondly the magnetic bearing is only to be engaged at certain frequencies. Specifically, the magnetic bearing is only to be switched on at frequencies where the amplitude of rotor vibration is reduced. For the rotor model referred to in this paper, with a magnetic bearing located at mid span, avoiding excessive vibration at the first critical speed requires engaging the magnetic bearing between around 85 and 160 Hz. The corresponding speed range on Figure 10 is highlighted. It can then be observed that at no point in the range where the bearing is actually active does the relative displacement come even close to the 1 mm boundary. Thus there is no collision.

VI. Practical Testing

A test rig has been designed to test the validity of the concept presented - schematic overviews are provided in Figures 11 and 12. This is currently under construction; when completed it should provide results to validate the numerical simulation. Initial testing is anticipated to consist of impulse testing of both simple and composite rotor arrangements to prove the difference in fundamental frequency. After that it is hoped to complete supercritical rotation tests to conclusively demonstrate the merit of the new topology. The rotor of the

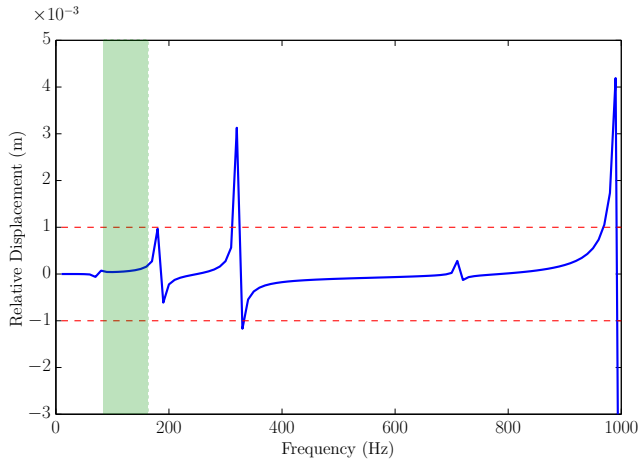

Figure 10. Displacement of magnetic bearing relative to corresponding location of rotor at various frequencies

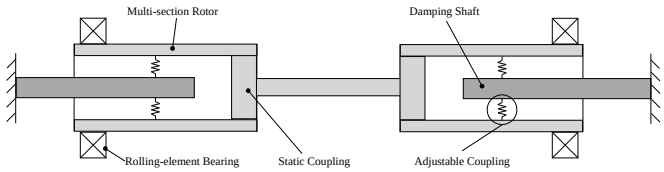

Figure 11. Schematic of novel rotor test rig

rig has been specially designed to allow supercritical rotation at relatively low speeds by building the rotor out of several sections, including a comparatively flexible middle section.

VII. Conclusions

A novel concept of coupling a rotor to a secondary shaft by way of internal-stator Active Magnetic Bearings has been proposed. Finite element modelling has been performed for such a rotor, and responses to an out-of-balance mass are plotted. It is clearly illustrated that it is possible to design a system whereby the critical speeds of the primary rotor are substantially altered by coupling it so a secondary shaft. Therefore by actively engaging and disengaging the magnetic couplings, it is possible to avoid the excessive vibration associated with the rotor's critical speeds. Furthermore, mode shape plots at rotor critical speeds are presented illustrating the difference in amplitude between the simple and coupled rotors, with maximum vibration amplitude reductions of around an order of magnitude observed. A design concept for a practicable laboratory-scale rig to confirm the finite element results is presented.

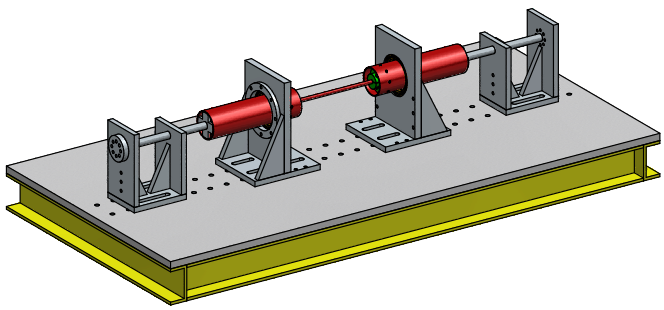

Figure 12. Pictorial overview of rotor test rig

VIII. Acknowledgements

The authors are grateful for the award of a James Dyson Foundation Studentship to support this research.

References

[1] FC Nelson. Rotor dynamics without equations. *International Journal of COMADEM*, 10(3):2, 2007.

[2] J Van De Vegte. Continuous automatic balancing of rotating systems. *IMechE Journal of Mechanical Engineering Science*, 6(3):264–269, 1964.

[3] AS Sekhar and Sarangi Debraj. Online balancing of rotors. In *National Conference on Mechanisms and Machines*, 2003.

[4] J Van de Vegte and RT Lake. Balancing of rotating systems during operation. *Journal of Sound and Vibration*, 57(2):225–235, 1978.

[5] J Van De Vegte. Balancing of flexible rotors during operation. *IMechE, Part C, Journal of Mechanical Engineering Science*, 23(5):257–261, 1981.

[6] RED Bishop and GML Gladwell. The vibration and balancing of an unbalanced flexible rotor. *IMechE Journal of Mechanical Engineering Science*, 1(1):66–77, 1959.

[7] RED Bishop. On the possibility of balancing rotating flexible shafts. *IMechE, Part C, Journal of Mechanical Engineering Science*, 24(4):215–220, 1982.

[8] Stephen W Dyer and Jun Ni. Adaptive influence coefficient control of single-plane active balancing systems for rotating machinery. *ASME Journal of Manufacturing Science and Engineering*, 123(2):291–298, 2001.

[9] Shiyu Zhou and Jianjun Shi. Active balancing and vibration control of rotating machinery: a survey. *Shock and Vibration Digest*, 33(4):361–371, 2001.

[10] Eric H Maslen and Gerhard Schweitzer. *Magnetic Bearings: Theory, Design, and Application to Rotating Machinery*. Springer, 2009.

[11] G. Schweitzer. Applications and research topics for active magnetic bearings. In *IUTAM Symposium on Emerging Trends in Rotor Dynamics*, pages 263–273. Springer, 2011.

[12] CR Burrows, MN Sahinkaya, and OS Turkay. An adaptive squeeze-film bearing. *ASME Journal of Tribology*, 106(1):145–151, 1984.

[13] Ilmar F Santos. Trends in controllable oil film bearings. In *IUTAM Symposium on Emerging Trends in Rotor Dynamics*, pages 185–199. Springer, 2011.

[14] Jinhao Qiu, Junji Tani, and Taekyu Kwon. Control of self-excited vibration of a rotor system with active gas bearings. *ASME Journal of Vibration and Acoustics*, 125(3):328–334, 2003.

[15] Ricardo C Simões, Valder Steffen, Johan Der Hagopian, and Jarir Mahfoud. Modal active vibration control of a rotor using piezoelectric stack actuators. *Journal of Vibration and Control*, 13(1):45–64, 2007.

[16] JL Nikolajsen, R Holmes, and V Gonhalekar. Investigation of an electromagnetic damper for vibration control of a transmission shaft. In *Institution of Mechanical Engineers Proceedings*, volume 193, 1979.

[17] MEF Kasarda, PE Allaire, RR Humphris, and LE Barrett. A magnetic damper for first-mode vibration reduction in multimass flexible rotors. *ASME Journal of Engineering for Gas Turbines and Power*, 112(4):463–469, 1990.

[18] MEF Kasarda, H Mendoza, RG Kirk, and A Wicks. Reduction of subsynchronous vibrations in a single-disk rotor using an active magnetic damper. *Mechanics Research Communications*, 31(6):689–695, 2004.

[19] Andrés Blanco Ortega, Francisco Beltrán Carbajal, Gerardo Silva, and Marco Antonio Oliver Salazar Navarro. Active vibration control of a rotor-bearing system based on dynamic stiffness control activo de vibraciones en un sistema rotor-chumaceras basado en la rigidez dinámica. *Revista Facultad de Ingeniería Universidad de Antioquia*, (55):125–133, 2010.

[20] HD Nelson and JM McVaugh. The dynamics of rotor-bearing systems using finite elements. *ASME Journal of Engineering for Industry*, 98:593, 1976.